

Structural Evolution and Phase Homologies for “Design” and Prediction of Solid-State Compounds

MERCOURI G. KANATZIDIS

*Department of Chemistry, Michigan State University,
East Lansing, Michigan 48824*

Received July 16, 2004

ABSTRACT

The challenge of designing solid state compounds with predicted compositions and structures could be partly met using concepts that employ phase homologies. Homologous series of compounds not only can place seemingly diverse phases into a single context; they can also forecast with high probability specific new phases. A homologous series is expressed in terms of a mathematical formula that is capable of producing each member. Within a homologous series, the type of fundamental building units and the principles that define how they combine remain preserved, and only the size of these blocks varies incrementally. In this Account, we present this approach by discussing a number of new homologies and generalize it for a wide variety of systems.

1. Introduction

Most research efforts in current solid-state chemistry are concerned with the design and prediction of new structures and materials.^{1–4} Progress has been considerable, and we have many cases in which “materials design” has been possible as, for example, simple isoelectronic elemental substitutions, the intercalation of species into solids, the synthesis of coordination solids based on aristotype solid-state structures, and the assembly of templated materials (see elsewhere in this issue). Nevertheless, in most cases the ability to broadly design and predict new phases is still limited.^{5,6} The predictability challenge in solid-state chemistry has two main facets. The first is how to synthesize a certain target phase and avoid unwanted phases, and the second is to predict compositions and structures that would be worth making.

It is often stated that molecular synthetic chemists (especially organic) can design and construct almost any target molecule in contrast to the solid-state chemist who

is unable to do so for solids. This comparison is not appropriate in most cases because small molecular organic units remain relatively intact throughout the reactions, so the goal is mainly to link one molecule to the next or to perform specific changes on functional groups. Unlike a molecular synthetic target, which can be built one step at a time and through several stable intermediates, the structures of solid-state materials are quasi-infinite, and they have to be constructed in most cases in a “single step” (one-pot synthesis). In other words, the structure assembly has to succeed the first time! A more fitting comparison is between the ability of molecular synthetic chemists to predict *how* molecules will orient and crystallize in the solid state vis-à-vis the ability of solid-state chemists to construct extended structures. To take the comparison even further, the organic chemist has very little ability to design complex organics for which there is no prior structural model and there is absence of intermediates that can lead to it. A case in point is C₆₀, C₇₀, etc., which cannot be reasonably designed and synthesized by step by step processes. They have to be prepared via “heat and beat” synthesis. In this context, the differences between the synthetic abilities of molecular synthetic and solid state chemists nearly vanish.

The most appealing challenge in solid-state chemistry has to do with predicting what structures would be stable and increase the odds of producing specific compounds. One elegant way is through the use of phase homologies, which can forecast modular compounds with predictable structure.

A homology is a series of structures built on the same structural principle with certain module(s) expanding in various dimension(s) by regular increments. This could be through the addition of a layer or row of atoms on a given module. If the module assembly principle is constant and only the module size and volume evolve, then we can view the series as a set of isorecticular compounds.⁷ A homologous series is expressed in terms of a mathematical formula that is capable of producing each member. It is a useful tool for designing compounds because it allows a modular classification of its members that concentrates on large scale structural features. These features are the modules and include large assemblages of atoms or coordination polyhedra or molecules. The modular classification of compounds requires a certain level of abstraction regarding the atomic occupancy and bonding details. The efficacy of a given homology lies in its property to generate countless structure types.

A structure can be assembled from one, two, or more kinds of modules. Generally, the modules in a homologous series of compounds are simple familiar units adopting archetypal structures or being excised from such structures (e.g., NaCl-type). The modules are often cluster blocks, infinite rods, or layers. To form each member, these modules recombine in various ways by the action of coordination chemistry principles or structure building operators, reflection twinning, glide reflection twinning,

Mercouri G. Kanatzidis was born in Thessaloniki, Greece, in 1957. He received his Ph.D. degree in chemistry from the University of Iowa in 1984, after obtaining a Bachelor of Science degree from Aristotle University in Greece. He is currently a University Distinguished Professor of Chemistry at Michigan State University where he has served since 1987. He was a postdoctoral research associate at the University of Michigan and Northwestern University from 1985 to 1987. He has been visiting professor at the University of Nantes (Institute des Materiaux Jean Rouxel) in 1996 and the University of Muenster in 2003. His research has generated seminal work in metal chalcogenide chemistry through the development of novel “solvents” for solid state synthesis including flux methods and hydrothermal and solvothermal techniques. He is also active in the field of new thermoelectric materials, the synthetic design of framework solids, intermetallic phases, and nanocomposite materials. The bulk of his work is described in the more than 420 research publications.

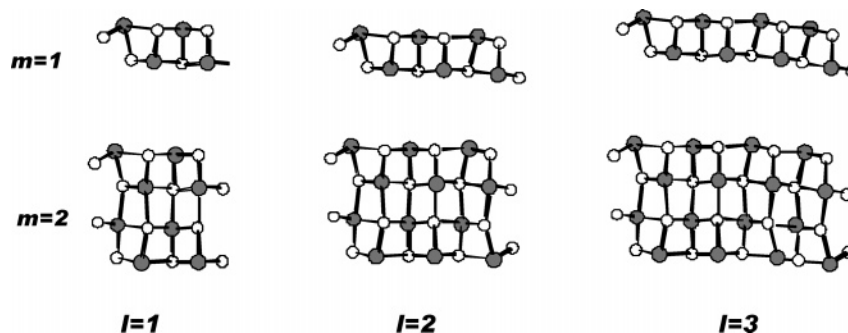


FIGURE 1. Fragments of the NaCl lattice that serve as modules for phase construction. The modules in this case have a cross section that changes (according to variables l and m), and they are infinite in length. Module evolution with l and m in the $[M_{1+l}Se_{2+l}]_{2m}[M_{2l+n}Se_{2+3l+n}]$ megaseries is depicted. The $l = 3$ module has not been found in compounds but is predicted to be stable in certain members of the series. Although $l = 1$ is the smallest l value for which we have known members, in principle members with $l = 0$ are also possible.

cyclic twinning, unit cell intergrowth, etc. These principles have been described in detail by Mackovicky.⁸

The name “homologous series” was coined to characterize chemical series that are expressed by general formulas and built on common structural principles,^{9,10} first in several complex metal oxide systems^{11–14} and later in any class including chalcogenides, intermetallics, etc.^{15–17} Several homologous series are known for sulfides. These include the gustavite–lillianite series¹⁸ the kobellite series,¹⁹ and the pavonite series²⁰ and others. The system BaQ/Fe₂Q₃ (Q = S, Se)²¹ was also found to define the fascinating 2D homologous series (BaQ)_n(Fe₂Q₃)_m. Another less investigated system that seems to form a homology is MnS/Y₂S₃.²²

To be of synthetic value, a series must have a structural building principle. It is not enough to have a general formula that combines two or more binary or ternary compounds to produce a compositional series, if every member has an unrelated crystal structure. For example, the system (Cu₂S)_n(Bi₂S₃)_m is only a compositional series, which can give target compositions for synthesis but lacks structural predictability, as members for various n and m values are unrelated structurally and thus cannot be predicted. Furthermore, to be of synthetic utility, it must be shown that at least some members of a homologous series must be designed and targeted for synthesis *after* their structure and composition is predicted from the general formula.

In a recent article, we discussed the concept of using phase homologies to achieve “design”²³ in solid-state chemistry based on a single series.²⁴ We outlined the concept of structural evolution and presented the new megaseries $A_m[M_{1+l}Se_{2+l}]_{2m}[M_{2l+n}Se_{2+3l+n}]$ (A = alkali or alkaline earth element; $M = M', M''$ main group metals) as a prime example. It is possible to predict not only the composition but also the structure of materials in the very broad system $A/M'/M''/Se$ while also achieving control in a solid-state reaction.

Here we expand upon this notion and present additional conceptual links between the existence of homologies and their implications for synthetic design in solid-state chemistry. Finally, we point to some general

implications that arise regarding design and prediction of compounds.

2. The Megaseries $A_m[M_{1+l}Se_{2+l}]_{2m}[M_{2l+n}Se_{2+3l+n}]$

One homologous series that demonstrates its predictive power in a spectacular way is $A_m[M_{1+l}Se_{2+l}]_{2m}[M_{2l+n}Se_{2+3l+n}]$. Because it presents three variable integers, l , m , and n , its breadth is wide and it impacts a large number of compounds. In this series, each member is realized by recombining two adjustable modules, $[M_{2l+n}Se_{2+3l+n}]$ and $[M_{1+l}Se_{2+l}]_{2m}$. The modules form a 3D framework with tunnels that accommodate the alkali ions (A_m). This series was recognized after several of its members had been discovered independently. After the homology was defined, many more members were prepared intentionally.

Both modules in this series are infinite rods sliced out of the NaCl lattice along different orientations and dimensions. There are several ways the NaCl lattice can be sectioned to produce the building fragments observed in the compounds discussed here. If the cut is made perpendicular to a certain direction, for example, [100] or [111], the fragment may be called NaCl¹⁰⁰-type or NaCl¹¹¹-type, respectively. In the general formula $A_m[M_{1+l}Se_{2+l}]_{2m}[M_{2l+n}Se_{2+3l+n}]$, $[M_{1+l}Se_{2+l}]_{2m}$ represents the NaCl¹⁰⁰-type module and $[M_{2l+n}Se_{2+3l+n}]$ represents the NaCl¹¹¹-type module. The size and shape of these building blocks are adjustable. While the thickness of the NaCl¹⁰⁰-type units is given by m , the shape of the NaCl¹¹¹-type units is controlled by n . The integer l sets the width (the number of MSe₆ octahedra) of *both* modules. Figures 1 and 2 illustrate the structures of the two types of modules and how they evolve systematically with the variables l , m , and n .

In homologous series with more than one variable, it is convenient to classify the different members by dividing them into subseries. For $A_m[M_{1+l}Se_{2+l}]_{2m}[M_{2l+n}Se_{2+3l+n}]$, it is useful to set one variable, for example, l , to 1, 2, etc. and then create subseries that are easier to handle. The organization of the modules into a three-dimensional structure follows the same motif for every member. The infinite rodlike NaCl¹¹¹-type units are linked side by side

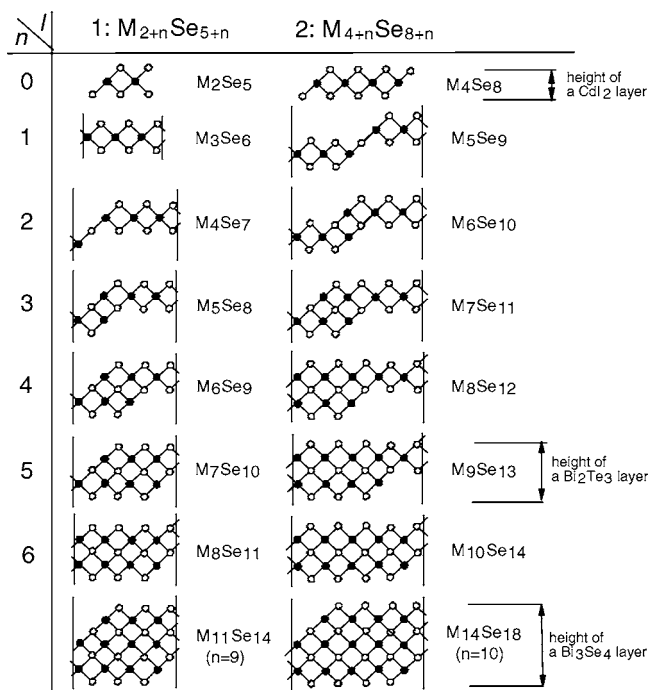


FIGURE 2. Module evolution with l and n in the $[M_{2+l}Se_{2+3+l}]$ part of the $A_m[M_{1+Se_2}]_m[M_{2+l}Se_{2+3+l}]$ megaserries. The structures of NaCl¹¹¹-type modules for various l and n values are depicted. For $l = 1$ and $n = 1$, we obtain the infinite CdI₂-type layer found in ABiSe₂.

in a trans fashion to form step-shaped slabs. Strong M–Se interactions between these layers and the NaCl¹⁰⁰-type rods form an anionic framework, creating tunnels running along the shortest crystallographic axis. Each formula corresponds to a unique structure type that can contain many ternary and quaternary members.²⁵

When $l = 1$, the superseries reduces to $A_m[M_4Se_6]_m[M_{2+n}Se_{5+m}]$. The isostructural phases Cs_{1.5–3x}Bi_{9.5+x}Se₁₅ and A_{1–x}M'_{1–x}Bi_{9+x}Se₁₅ ($A = Rb, Cs; M' = Sn, Pb$)²⁶ are members of this series with $m = 1$ and $n = 4$. Figure 3 depicts a projection of this structure type along the b axis. The NaCl¹¹¹-type fragments, the $[M_6Se_9]$ modules, are three BiSe₆ octahedra wide and two octahedra thick, and they are linked by two adjacent identical modules sharing an octahedron face to form a step-shaped layer. This kind of linkage for the NaCl¹¹¹-type modules is typical for $n = 4$. An identical arrangement of these modules to a step-shaped layer is also found for A_{1–x}M'_{3–x}Bi_{11+x}Se₂₀,²⁷ A_{1+x}–

M'_{3–2x}Bi_{7+x}Se₁₄, and K_{2.5}Bi_{8.5}Se₁₄.²⁸ In these members, where ($l = 2$), the NaCl¹¹¹-type units are wider by one BiSe₆ octahedron than those in Cs_{1.5–3x}Bi_{9.5+x}Se₁₅ and A_{1–x}–M'_{1–x}Bi_{9+x}Se₁₅ ($l = 1$).

In the case where $l = 2$, the general formula becomes $A_m[M_6Se_8]_m[M_{4+n}Se_{8+n}]$. The known structure types for $l = 2$ with $m = 1$ and 2 are organized in Figure 4, which shows how higher members evolve from lower ones by adding MSe equivalents to the initial NaCl¹¹¹-type layers; see, for example, in Rb_{1+x}Sn_{1–2x}Bi_{7+x}Se₁₂ ($n = 0$). Here the $[M_4Se_8]$ layer consists of one octahedron high and four octahedra wide fragments. The NaCl¹¹¹-type module here is so thin it resembles a “cut out” of a CdI₂-type layer for $n = 0, 2$. Successive addition of MSe equivalents to these structural modules generates thick NaCl¹¹¹-type units that begin to resemble the Bi₂Te₃-type ($n = 4, 5, 6$) and the Bi₃Se₄-type ($n = 10$) structures. This process can continue indefinitely creating new and predictable structure types. The challenge is how to stabilize each member in pure phase, and this may occupy the synthetic chemist for some time as the l, m , and n become large. This is not necessarily a failure of the homology approach. Conceptually this challenge is equivalent to trying to stabilize different and arbitrary molecular weights in a given polymer system. It is not easy and can be anywhere from achievable to time-consuming to impossible.

Four different structure types with $m = 1$ are known, A_{1–x}M'_{3–x}Bi_{11+x}Se₂₀, A_{1–x}M'_{4–x}Bi_{11+x}Se₂₁,²⁹ A_{1–x}M'_{5–x}Bi_{11+x}Se₂₂,³⁰ and A_{1–x}Sn_{9–x}Bi_{11+x}Se₂₆³¹ ($A = K, Rb, Cs; M' = Sn, Pb$) adopted by every possible combination of A and M' . Only A_{1–x}Sn_{9–x}Bi_{11+x}Se₂₆ is an exception, where no Pb analogues have been prepared.³² These four types of phases exhibit the same NaCl¹⁰⁰-type unit, $[M_6Se_8]$, that is one octahedron thick in the direction perpendicular to the step-shaped NaCl¹¹¹-type layers and three octahedra wide in the direction parallel to the layers.

Within the subseries AM_{10+n}Se_{16+n} ($l = 2, m = 1$) structural evolution takes place by varying only the size and shape of the NaCl¹¹¹-type module $[M_{4+n}Se_{8+n}]$ according to the specific values of the integer n . In A_{1–x}M'_{3–x}Bi_{11+x}Se₂₀ ($n = 4$) the NaCl¹¹¹-type module is four octahedra wide and two octahedra thick, see Figure 4. Condensation of these units via one octahedron edge results in a step-shaped layer of the formula $[M_8Se_{12}]$ ($n = 4$). In contrast, the NaCl¹¹¹-type blocks for $n = 5$ are two octahedra thick

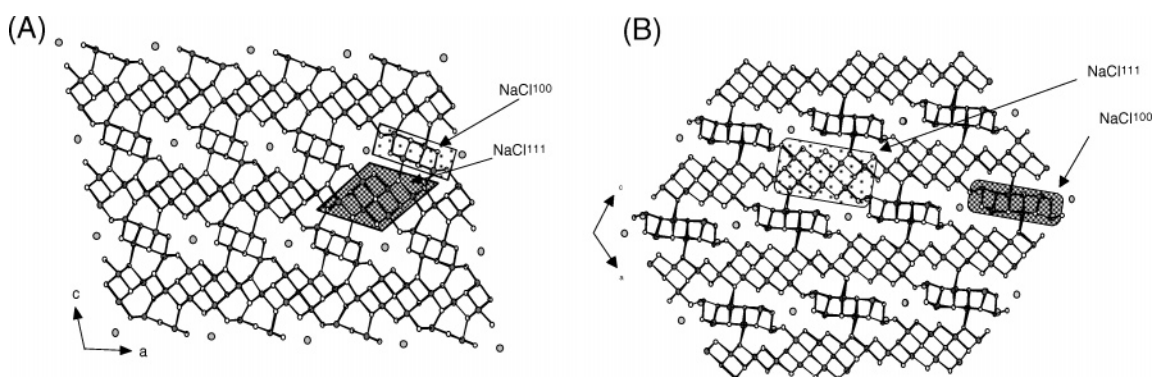


FIGURE 3. The structure of (A) A_{1–x}M'_{1–x}Bi_{9+x}Se₁₅ and (B) A_{1–x}M'_{3–x}Bi_{11+x}Se₂₀. The difference between the two phases is values of l .

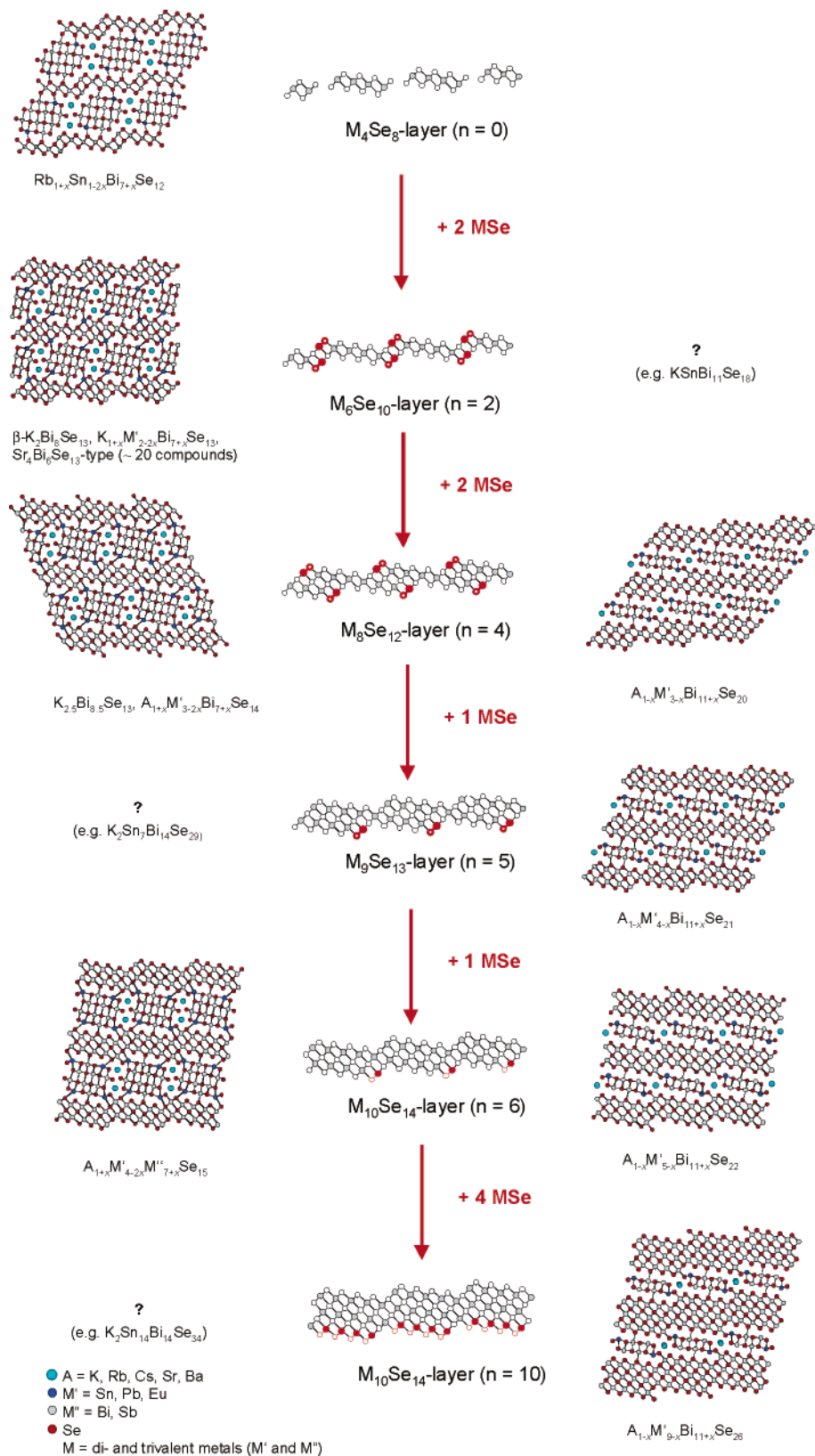
The subseries $A_m[M_6Se_8]_m[M_{4+n}Se_{8+n}]$ for $l = 2$ 

FIGURE 4. A member-generating scheme illustrating successive additions of MSe units to a M_4Se_8 layer in the homologous subseries $A_m[M_6Se_8]_m[M_{4+n}Se_{8+n}]$ for $l = 2$. Small white spheres denote Se, large light-gray spheres A, and middle-gray spheres M. Question marks indicate predicted but as of yet undiscovered compositions.

but five octahedra wide. Their connection point is defined by a central octahedral *M* atom. However, the same building units, which are also offset, are joined via an octahedron edge in $A_{1-x}M'_{5-x}Bi_{11+x}Se_{22}$ ($n = 6$), Figure 4. The same kind of linkage is also found in $A_{1-x}Sn_{9-x}Bi_{11+x}Se_{26}$ ($n = 10$), but the modules are now three octahedra thick. By addition of 4 equiv of MSe to $A_{1-x}M'_{5-x}Bi_{11+x}Se_{22}$ ($n = 6$), the thickness of the slabs defined by the $NaCl^{111}$ units increases to the point that it now resembles a layer of the Bi_3Se_4 structure type instead of a layer of the Bi_2Te_3 -type found for $n = 4-6$. Similar to $A_{1-x}M'_{1-x}Bi_{9+x}Se_{15}$, the alkali atoms are situated in tricapped trigonal prismatic sites in the circular tunnels running along the *b* axis of all the structures with $l = 2$ and $m = 1$. The charge-balanced formulas, for example, $A_{1-x}M'_{5-x}Bi_{11+x}Se_{22}$, indicate vacancies on the alkali sites that are compensated by positional disorder of di- and trivalent metals within the anionic framework.

When $m = 2$, the height of the $NaCl^{100}$ -type modules doubles resulting in a $[M_{12}Se_{16}]$ block that is three octahedra wide in the direction parallel to the $NaCl^{111}$ -type layers and two octahedra thick perpendicular to this direction giving the subseries $AM_{8+n}Se_{12+n}$. By comparison with the structures where $m = 1$, which feature tunnels with only one tricapped trigonal crystallographic site, the thicker modules ($m = 2$) create double tunnels with two tricapped trigonal prismatic sites per unit cell. These sites are usually fully occupied by alkali ions when $m = 2$, in contrast to the structures with $m = 1$ where a statistical disorder is always found on the tricapped prismatic sites. Alkali atoms also are found on the metals sites in the edges of the $NaCl^{100}$ -type module disordered with the di- and trivalent metals of the anionic framework. To express the variable composition of these phases, the formulas are written as, for example, $A_{1+x}M'_{4-2x}Bi_{7+x}Se_{15}$.

$Rb_{1+x}Sn_{1-2x}Bi_{7+x}Se_{12}$ is the first member of the subseries $A_2M_{16+n}Se_{24+n}$ for $l = 2$, $m = 2$, and $n = 0$. The structure is shown in Figure 4. Successively adding 2 equiv of MSe leads to the compounds $K_{1+x}M'_{2-2x}Bi_{7+x}Se_{13}$, $K_{1+x}M'_{3-2x}Bi_{7+x}Se_{14}$, and $K_{1+x}M'_{4-2x}Bi_{7+x}Se_{15}$, which vary in the size and shape of the $NaCl^{111}$ -type module while the $NaCl^{100}$ -type module (i.e., the $[M_{12}Se_{16}]$ block) remains unchanged. $Rb_{1+x}Sn_{1-2x}Bi_{7+x}Se_{12}$ features "isolated" $NaCl^{111}$ -type modules, which represent four octahedra wide ribbons "cut out" of a CdI_2 -type layer arranged in a step-shaped fashion. Linkage of these fundamental building units creates a three-dimensional framework via strong M–Se interactions that complicates a strict assignment of the atoms to the two different modules. This particular $NaCl^{111}$ -type module has no correspondence in the subseries $AM_{10+n}Se_{16+n}$ for $m = 1$. For $n = 0$, this general formula predicts $AM_{10}Se_{16}$, and a charge-balanced composition would be $SrBi_{10}Se_{16}$.

$A_{1+x}M'_{2-2x}M''_{7-x}Se_{13}$ ($l = 2$, $m = 2$, $n = 2$) defines the so-called $Sr_4Bi_6Se_{13}$ structure type,³³ a very stable architecture that is adopted by many ternary and quaternary systems including $K_2Bi_8Sb_3Se_{13}$,³⁴ $Sr_2Pb_2Bi_6Se_{13}$,³⁵ $Ba_2Pb_2Bi_6Sb_3$,³⁵ $Ba_4Bi_6Se_{13}$,³⁵ $Ba_3M'Bi_6Se_{13}$,³⁶ ($M' = Sn, Pb$), $Eu_2Pb_2Bi_6Se_{13}$,³⁷

and the solid solutions $K_2Bi_{8-x}Sb_xSe_{13}$ for $0 \leq x \leq 8$.³⁸ The main characteristic is that the $[Bi_6Se_{13}]^{8-}$ part of the structure remains intact while the Sr^{2+} positions can be substituted with a variety of similarly sized ions, Ba^{2+} , K^+ , Bi^{3+} , Pb^{2+} , etc., so long as they maintain electroneutrality.

Since these compounds have integers of $l = 2$ and $n = 2$, they all exhibit the same $NaCl^{111}$ -type module, which is six octahedra wide and linked via a common edge to form a step-shaped layer, Figure 2. These relatively thin layers interact strongly with the $NaCl^{100}$ -type units resulting in a rigid three-dimensional framework in which the distribution and assignment of various metal atoms in the different building units, especially in the interconnection points can get ambiguous. Due to the nearly square cross section of the $NaCl^{100}$ -type rods ($m = 2$), the tunnels forming along the short *b* axis acquire an elongated cross section creating two tricapped trigonal prismatic sites that accommodate the alkali, alkali earth, Sr, or Eu atoms in the different phases of the $Sr_4Bi_6Se_{13}$ structure.

Adding 2 equiv of MSe to the $NaCl^{111}$ -type fragments of the $Sr_4Bi_6Se_{13}$ structure gives the $[M_8Se_{12}]$ module. This building unit is also present in the same step-shaped layers of $A_{1-x}M'_{3-x}Bi_{11+x}Se_{20}$ ($A = K, Rb, Cs$; $M' = Sn, Pb$). Combining these with the $NaCl^{100}$ -type blocks found in the $Sr_4Bi_6Se_{13}$ and $Rb_{1+x}Sn_{1-2x}Bi_{7+x}Se_{12}$ -type motifs defines a different structure type, which is adopted by α - $K_{2.5}Bi_{8.5}Se_{14}$,²⁸ γ - $K_2Bi_8Se_{13}$,³⁹ a defect variant of α - $K_{2.5}Bi_{8.5}Se_{14}$, and $A_{1+x}M'_{3-2x}Bi_{7+x}Se_{14}$ ($A = K, Cs$; $M' = Sn, Pb$). So far we could not obtain the Rb analogue of $A_{1+x}M'_{3-2x}Bi_{7+x}Se_{14}$. For these phases, $l = 2$, $m = 2$, and $n = 4$. Although the compounds $Rb_{2.5-x}M'_{2x}Bi_{8.5-x}Q_{14}$ ($M' = Pb, Sn, Eu$; $Q = S, Se$) fit the general formula of the homologous series for $l = 2$, $m = 2$, and $n = 4$, they are not isostructural to α - $K_{2.5}Bi_{8.5}Se_{14}$. Instead they adopt the dissimilar structure type of β - $K_{2.5}Bi_{8.5}Se_{14}$.⁴⁰ In this case, we can see that the homology predicts only the correct composition but fails to accurately forecast the crystal structure.

Climbing the evolutionary ladder higher, we obtain the $A_{1+x}M'_{4-2x}M''_{7-x}Se_{15}$ structure type⁴¹ by adding 2 equiv of MSe to the α - $K_{2.5}Bi_{8.5}Se_{14}$ -type, 4 equiv of MSe to the $Sr_4Bi_6Se_{13}$ -type, or 6 equiv of MSe to the $Rb_{1+x}Sn_{1-2x}Bi_{7+x}Se_{12}$ -type, respectively. This structural evolution causes the growth of the $NaCl^{111}$ -type modules, which form the step-shaped layers. At the same time, the $NaCl^{100}$ -type block remains invariant for all structure types. Now the variables are $l = 2$, $m = 2$, and $n = 6$. The $A_{1+x}M'_{4-2x}M''_{7-x}Se_{15}$ -type is realized for $A_{1+x}M'_{4-2x}Bi_{7+x}Se_{15}$ ($A = K, Rb$; $M' = Sn, Pb$), $A_{1+x}Pb_{4-2x}Sb_{7+x}Se_{15}$, and $Ba_{2+x}Pb_{4-x}Bi_6Se_{15}$. Figure 5 illustrates the structure of $Ba_{2+x}Pb_{4-x}Bi_6Se_{15}$ projected down the *b* axis. To better see the compositional relationship of this compound to its other analogues, the formula can be written ideally as $Ba[BaPb_3][PbBi_6]Se_{15}$. The tricapped trigonal prismatic sites are exclusively occupied by Ba or alkali metal atoms, while the two bicapped trigonal prismatic sites reveal disorder of alkali/alkaline earth metal and the di-/trivalent metal atom often causing split positions at those sites. Since $n = 6$, these compounds reveal the same $NaCl^{111}$ -type layers as in $A_{1-x}M'_{5-x}Bi_{11+x}Se_{22}$

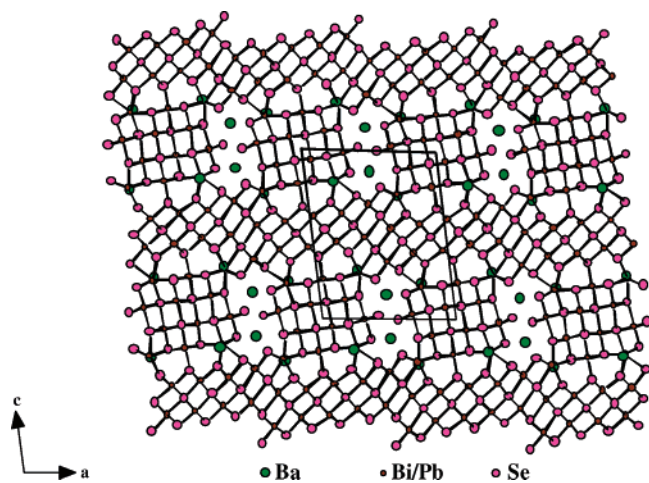


FIGURE 5. The structure of $\text{Ba}_{2+x}\text{Pb}_{4-x}\text{Bi}_6\text{Se}_{15}$ ($l = 2$, $m = 2$, $n = 6$).

($l = 2$, $m = 1$, $n = 6$). The alkali/alkaline earth metal is found in the tricapped trigonal prismatic sites and also disordered with the divalent metal at the periphery of the NaCl^{100} -type module on the bicapped trigonal prismatic sites. In addition to the many quaternary members of the homologous series with $l = 2$, $m = 2$, and $n = 2$ or 4, the ternary analogues $\text{A}_3\text{Bi}_9\text{Se}_{15}$ (i.e., ABi_3Se_5 ⁴²) are also predicted by the series $\text{A}_m[\text{M}_{1+l}\text{Se}_{2+l}]_{2m}[\text{M}_{2+n}\text{Se}_{2+3l+n}]$.

It is clear that the general formula of the megaseries $\text{A}_m[\text{M}_{1+l}\text{Se}_{2+l}]_{2m}[\text{M}_{2+n}\text{Se}_{2+3l+n}]$ (or any series) has predictive character. Varying the integers l , m , and n independently causes structural evolution in three independent dimensions. Therefore we are able to predict both the structure and composition of a vast number of new compounds that fit the general formula. According to the series, we can generate, for example, the charge-balanced formula $\text{A}_2\text{-Sn}_{12}\text{Bi}_{14}\text{Se}_{34}$ for the following values of the integer: $l = 2$, $m = 2$, and $n = 10$. We expect this compound to reveal the same kind of NaCl^{111} -type modules as found in $\text{ASn}_9\text{-Bi}_{11}\text{Se}_{26}$, but being higher in the evolutionary ladder, the NaCl^{100} -type modules are twice as thick, see Figure 6. Already we successfully targeted several compounds for synthesis *after* their composition and structure had been predicted by the general formula, namely, $\text{A}_{1-x}\text{M}'_{3-x}\text{-Bi}_{11+x}\text{Se}_{20}$, $\text{A}_{1+x}\text{M}'_{3-2x}\text{Bi}_{7+x}\text{Se}_{14}$, $\text{K}_{1+x}\text{M}'_{2-2x}\text{Bi}_{7+x}\text{Se}_{13}$, and $\text{A}_{1-x}\text{Sn}_{9-x}\text{Bi}_{11+x}\text{Se}_{26}$ ($\text{A} = \text{K}, \text{Rb}, \text{Cs}$; $\text{M}' = \text{Sn}, \text{Pb}$). In general, modifying the three independent integers l , m , and n provides three different ways to change *predictably* the structure of known compounds. Figure 4 depicts some of these ways whereby adding or subtracting MSe equivalents causes growth or shrinkage of the NaCl^{111} -type modules to create modules for different step-shaped layers.

Based on the modular construction of all members of the superseries, the design of novel hypothetical structures, prediction of their composition, and even simulation of their characteristic diffraction pattern become possible. For example, new members with $l = 1, 3, \dots$ or $m = 3, 4$ could be envisioned and rationally targeted for synthesis.

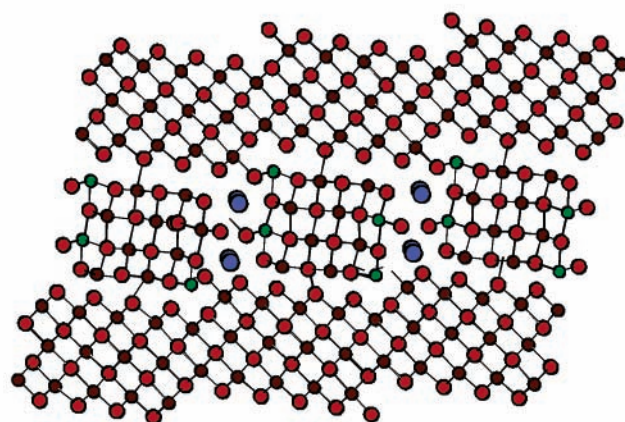
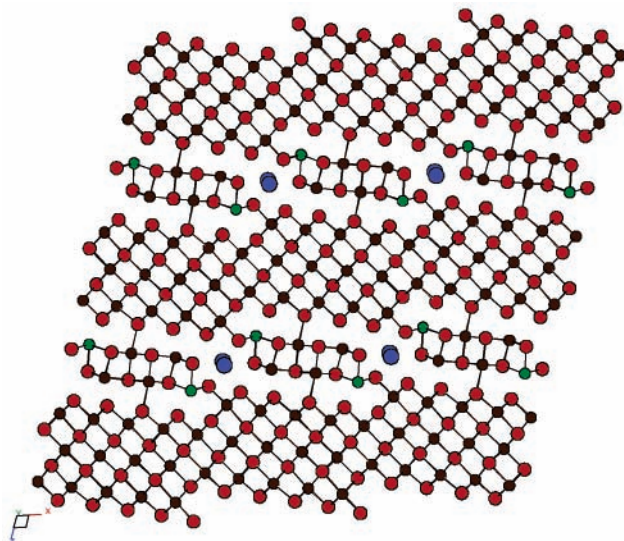


FIGURE 6. Comparison between $\text{ASn}_9\text{Bi}_{11}\text{Se}_{26}$ ($l = 2$, $m = 1$, $n = 10$) and the predicted $\text{A}_2\text{Sn}_{12}\text{Bi}_{14}\text{Se}_{34}$ ($l = 2$, $m = 2$, $n = 10$).

3. The Series $[(\text{PbSe})_5]_n[(\text{Bi}_2\text{Se}_3)_3]_m$

Another interesting homology was found in the $\text{PbSe}/\text{Bi}_2\text{Se}_3$ system. The homology can be depicted as $[(\text{PbSe})_5]_n - [(\text{Bi}_2\text{Se}_3)_3]_m$ and generates a series of compounds composed of two types of infinite slabs. One type is a slice out of the PbSe (NaCl^{100}) lattice in which the cut is made perpendicular to the (100) axis, and therefore it has an ideal tetragonal symmetry. In principle, it can have a variable thickness that is controlled by the value of n . The other type of slab is generated by a cut made perpendicular to the (111) axis and creates a hexagonal Bi_2Se_3 layer. The value of m indicates how many of these Bi_2Se_3 layers exist in the repeating unit of the structure. Adjacent Bi_2Se_3 layers interact via van der Waals gaps in the same way observed in the structure of Bi_2Se_3 (an end member with $n = 0$ and $m = \infty$). The two types of slabs stack along one direction to generate the crystal structure, Figure 7.

This mode of assembly is simple and similar to that found in the well-known class of misfit compounds that are another example of phase homology, $[(\text{MQ})_m]_{1+x}(\text{TQ}_2)_n$.^{43,44} The MQ part is an approximate tetragonal layer often called the Q sublattice (not to be confused with the chalcogen atoms) and the TQ_2 sublattice is a hexagonal

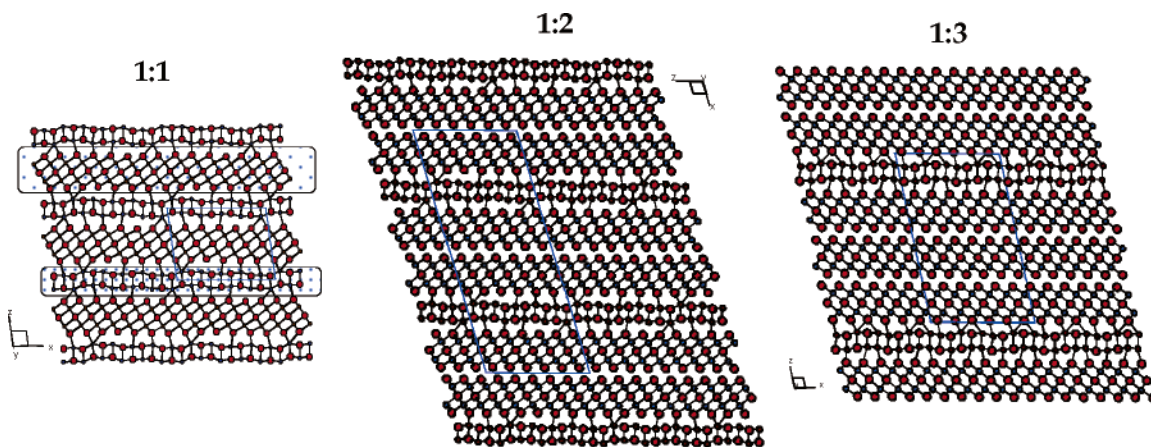


FIGURE 7. The structure of three members of the $[(\text{PbSe})_5]_n[(\text{Bi}_2\text{Se}_3)_3]_m$ homology: left, $\text{Pb}_5\text{Bi}_6\text{Se}_{14}$ ($m = 1, n = 1$); middle, $\text{Pb}_5\text{Bi}_{12}\text{Se}_{23}$ ($m = 1, n = 2$); right, $\text{Pb}_5\text{Bi}_{18}\text{Se}_{32}$ ($m = 1, n = 3$).

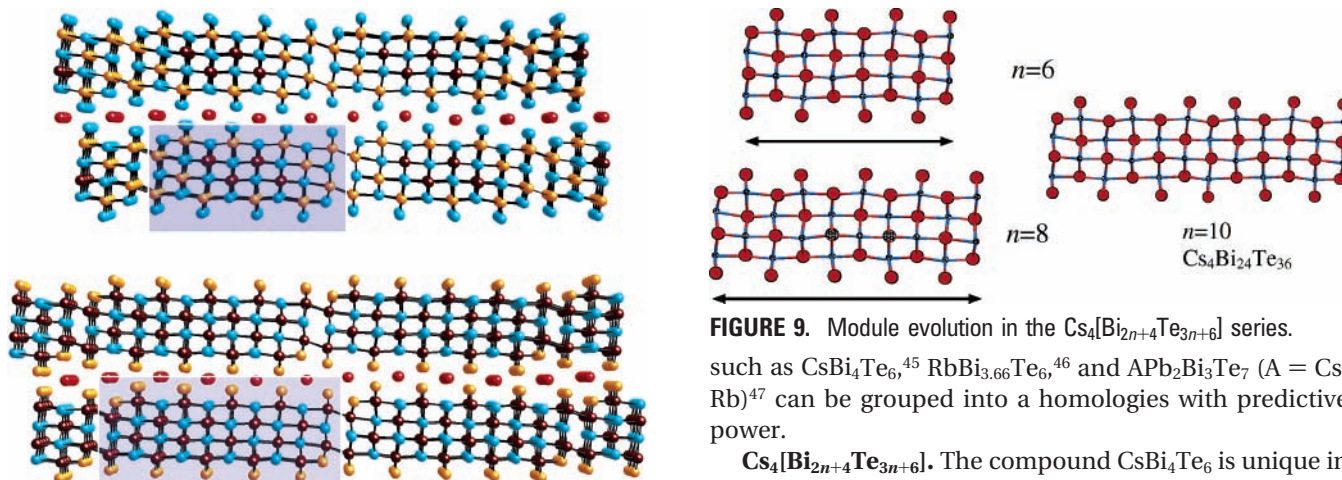


FIGURE 8. Comparison of the structures of CsBi_4Te_6 (top) and $\text{Cs}_4\text{Bi}_{20}\text{Te}_{30-x}\text{Se}_x$ (bottom).

layer called the H-part. They are called misfit because the periodicities of the MQ and TQ_2 parts do not match exactly. This results in incommensurate superstructures built from an alternate stacking of two different layered entities (sublattices Q and H), giving them a composite character (i.e., intergrowth compounds). The first two members in this series are $\text{Pb}_5\text{Bi}_6\text{Se}_{14}$ ($m = 1, n = 1$) and $\text{Pb}_5\text{Bi}_{12}\text{Se}_{23}$ ($m = 1, n = 2$), and it is possible that these too are misfit compounds. The mineral canizzarite is a member of this series. The compound $\text{Pb}_5\text{Bi}_{18}\text{Se}_{32}$ ($m = 1, n = 3$) was anticipated as the next member of the series with ($m = 1, n = 3$) and successfully targeted for synthesis. In all three of these compounds, $m = 1$. Because this set is now a homology, it is easy to anticipate specific new phases with $m = 2$ or 3 in which the tetragonal (NaCl^{100}) part is thicker. Future work should reveal additional predicted members.

4. Homologous Series in the Telluride Systems

In sharp contrast to the selenide compounds discussed above, isostructural Te analogues could not be prepared. Rather, the A/Bi/Te and A/Pb/Bi/Te systems give rise to different structure types. Several interesting compounds

such as CsBi_4Te_6 ,⁴⁵ $\text{RbBi}_{3.66}\text{Te}_6$,⁴⁶ and $\text{APb}_2\text{Bi}_3\text{Te}_7$ ($A = \text{Cs, Rb}$)⁴⁷ can be grouped into a homologies with predictive power.

$\text{Cs}_4[\text{Bi}_{2n+4}\text{Te}_{3n+6}]$. The compound CsBi_4Te_6 is unique in that it has anionic $[\text{Bi}_4\text{Te}_6]$ rods, which are parallel to each other and are linked with Bi–Bi bonds at 3.238(1) Å. This forms slabs that alternate with layers of Cs^+ ions to form the structure, Figure 8. CsBi_4Te_6 is a reduced compound that derives from Bi_2Te_3 by adding electrons that localize on the Bi atoms. The $[\text{Bi}_4\text{Te}_6]$ rod is the basic module of the compound, and in principle, it can be imagined to vary in width or in height. Indeed, we discovered a second compound, $\text{Cs}_4\text{Bi}_{20}\text{Te}_{30-x}\text{Se}_x$, that is related to CsBi_4Te_6 , and it too represents reduced $\text{Bi}_2\text{Te}_{3-x}\text{Se}_x$. In fact the two systems could be homologues since their structure is based on the same assembly principle where parallel rods of $[\text{Bi}_x\text{Te}_y]$ are linked side by side with Bi–Bi bonds, except that the rods are now wider, that is, $[\text{Bi}_5\text{Te}_{7.5}]_2$, Figure 8. Together the two compounds forecast the existence of a possible homology of the type $\text{Cs}_4[\text{Bi}_{2n+4}\text{Te}_{3n+6}]$ with possible predicted phases $\text{Cs}_4\text{Bi}_{24}\text{Te}_{36}$ ($n = 10$), $\text{Cs}_4\text{Bi}_{28}\text{Te}_{42}$ ($n = 12$), and $\text{Cs}_4\text{Bi}_{12}\text{Te}_{18}$ ($n = 4$). The module evolution in such a series is depicted in Figure 9, for $n = 6, 8$, and 10.

$\text{CsPb}_m\text{Bi}_3\text{Te}_{5+m}$. Investigations in the system A/Pb/Bi/Te led to $\text{CsPbBi}_3\text{Te}_6$, $\text{CsPb}_2\text{Bi}_3\text{Te}_7$, $\text{CsPb}_3\text{Bi}_3\text{Te}_8$, and $\text{CsPb}_4\text{Bi}_3\text{Te}_9$.⁴⁸ The compounds adopt layered structures built up of anionic slabs with progressively increasing thickness. These slabs can be viewed as fragments excised from {PbTe}-type (i.e., NaCl) structure with the thickness of 4, 5, 6, and 7 {PbTe} monolayers. This family offers a brand-

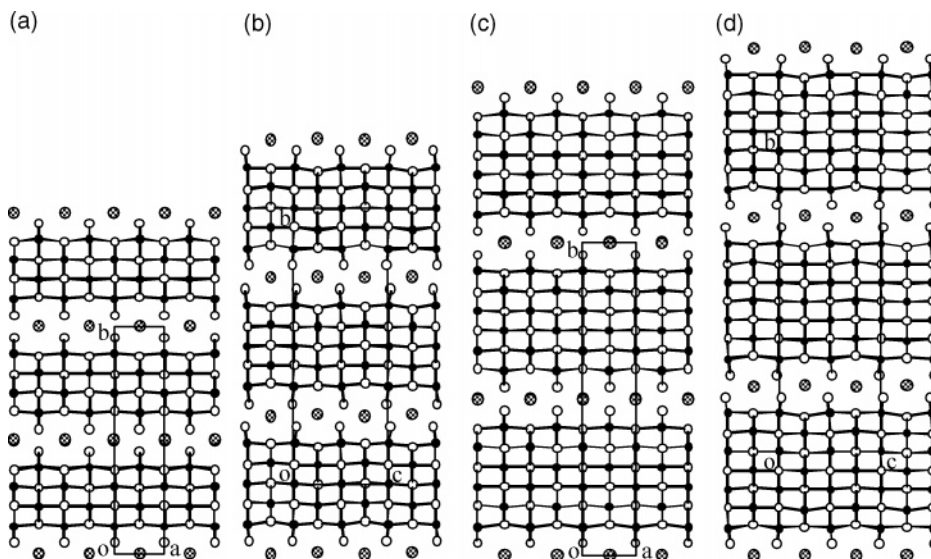


FIGURE 10. Structure sequence as a function of m in the homologous series $\text{CsPb}_m\text{Bi}_3\text{Te}_{5+m}$: (a) $\text{CsPbBi}_3\text{Te}_6$, $m = 1$; (b) $\text{CsPb}_2\text{Bi}_3\text{Te}_7$, $m = 2$; (c) $\text{CsPb}_3\text{Bi}_3\text{Te}_8$, $m = 3$; (d) $\text{CsPb}_4\text{Bi}_3\text{Te}_9$, $m = 4$. $\text{RbBi}_{3.66}\text{Te}_6$ has the structure of panel a.

new homologous series, $\text{CsPb}_m\text{Bi}_3\text{Te}_{5+m}$ ($m = 1-4$). The members with $m = 1$ and 2 were discovered first and suggested the possible existence of a homology in this system. The last two members however were predicted and successfully targeted for synthesis. The structures consist of infinite $[\text{Pb}_m\text{Bi}_3\text{Te}_{5+m}]^-$ slabs separated with Cs^+ cations, see Figure 10.

The crystallographically distinct metal sites, M, in the $[\text{M}_{m+3}\text{Te}_{5+m}]^-$ slab are octahedrally coordinated with Te atoms. Both Bi^{3+} and Pb^{2+} ions occupy the M sites in the four structures. This mixed occupancy behavior also occurs in the isostructural Sn analogues. The $[\text{PbBi}_3\text{Te}_6]^-$ slab can be viewed as a fragment excised from PbTe-type structure along the $[110]$ direction with a thickness of four $\{\text{PbTe}\}$ monolayers, see Figure 11a. The structure of $\text{CsPb}_2\text{Bi}_3\text{Te}_7$ has thicker $[\text{Pb}_2\text{Bi}_3\text{Te}_7]^-$ slabs, as displayed in Figure 10b. The $[\text{Pb}_2\text{Bi}_3\text{Te}_7]^-$ slab is also a fragment excised from PbTe-type structure with five $\{\text{PbTe}\}$ monolayers, that is, one monolayer thicker than the slab in Figure 11a, Figure 11(b). Remarkably, this architecture can sustain thicker anionic slabs to give $\text{CsPb}_3\text{Bi}_3\text{Te}_8$ and $\text{CsPb}_4\text{Bi}_3\text{Te}_9$ structures, Figure 10, panels c and d. The anionic slabs in Figure 10c,d are also fragments of the PbTe-type structure with six and seven $\{\text{PbTe}\}$ monolayers, Figure 11, panels c and d. As a result, the crystallographic axes perpendicular to the layers systematically increase with the number of PbTe monolayers.

The structure of the ternary $\text{RbBi}_{3.66}\text{Te}_6$ is the same as that of $\text{CsPbBi}_3\text{Te}_6$ and is composed of $[\text{Rb}_{0.34}\text{Bi}_{3.66}\text{Te}_6]$ layers separated by Rb atoms, see Figure 10a. The Rb and Bi atoms in this layer are statistically disordered (i.e., mixed occupancy). The $[\text{Rb}_{0.34}\text{Bi}_{3.66}\text{Te}_6]$ layer has a similar array of $[\text{MTe}_6]$ octahedra to that of Bi_2Te_3 and can be considered a two-dimensional fragment excised out of the NaCl structure. The Rb atoms are sandwiched between the $[\text{Rb}_{0.34}\text{Bi}_{3.66}\text{Te}_6]$ layers, and their sites are filled only at the 66.7% level. Therefore, this compound contains vacancies and can be formulated as $\text{Rb}_{0.66}[\text{Rb}_{0.34}\text{Bi}_{3.66}\text{Te}_6]$.

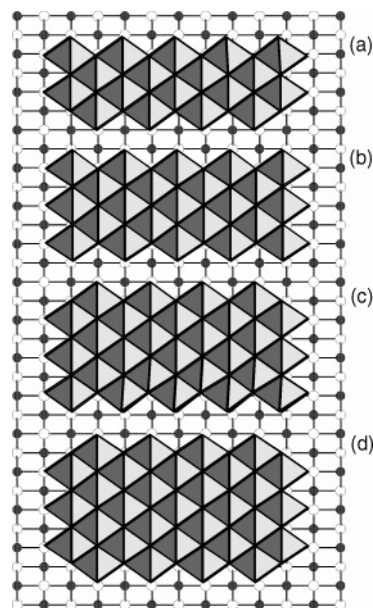


FIGURE 11. A view of the PbTe structure along the $[110]$ direction. The anionic slabs in the structures of $\text{CsPbBi}_3\text{Te}_6$, $\text{CsPb}_2\text{Bi}_3\text{Te}_7$, $\text{CsPb}_3\text{Bi}_3\text{Te}_8$, and $\text{CsPb}_4\text{Bi}_3\text{Te}_9$ are fragments excised from this lattice with (a) 4, (b) 5, (c) 6, and (d) 7 $\{\text{PbTe}\}$ monolayers thick, respectively.

5. Concluding Remarks

The potential of phase homologies for designing new solid-state compounds goes far beyond the few examples highlighted here. Many reported compounds, now considered unrelated, could be classified and placed in the context of phase homologies. Once homologies have been identified new member phases can be predicted. Not only will this promote better understanding of their interrelationships, but it could enhance our predictive ability and bring us closer to the goal of “rational design” for many classes of compounds. Phase homologies could prove to be an important design tool for bulk solid-state materials. Because the structures of new members are fully predictable, theoretical studies (e.g., property calculations,

simulations) can be performed on them to assess whether such phases are worth pursuing from the synthesis perspective.

It is remarkable that in the $A/M'/Bi/Q$ ($A = K, Rb, Cs$; $M' = Sn, Pb$; $Q = Se, Te$) system alone exist several homologous series. One is $A_m[M_{1+l}Se_{2+l}l_{2m}[M_{2+l+n}Se_{2+3l+n}]$ and captures a substantial fraction of compounds possible in various $A/M'/Se$ and $A/M'/M'/Se$ combinations. The others are $[(PbSe)_5]_n[(Bi_2Se_3)_3]_m$, $Cs_4[Bi_{2n+4}Te_{3n+6}]$, and $APb_mBi_3Te_{5+m}$. Each series presents compositional variables that control structural evolution in various spatial dimensions. The construction of each member of the homologous series is modular and achieved by one or more adjustable building units. Because many compounds in our work have been successfully targeted for preparation after their structure and composition was predicted by the general formula, we propose that the special value of these homologous series is that they have predictive character. In essence, homologous series amount to "compound generating machines"! Finally, homologies could help understand the relationships between crystal structure, electronic band structure, and composition across successive members of the series.

We thank the Office of Naval Research for financial support of this research.

References

- Jansen, M. A Concept for Synthesis Planning in Solid-State Chemistry. *Angew. Chem., Int. Ed.* **2002**, *41*, 3747–3766.
- DiSalvo, F. J. Challenges and Opportunities in Solid State Chemistry. *Pure Appl. Chem.* **2000**, *72*, 1799–1807.
- DiSalvo, F. J. Solid State Chemistry. *Solid State Commun.* **1997**, *102*, 79–85.
- Yaghi, O. M.; O'Keeffe, M.; Kanatzidis, M. G. Design of Solids from Molecular Building Blocks: Golden Opportunities for Solid State Chemistry. *J. Solid State Chem.* **2000**, *152*, 1–2.
- O'Keeffe, M.; Eddaoudi, M.; Li, H.; Reineke, T.; Yaghi, O. M. Frameworks for Extended Solids: Geometrical Design Principles. *J. Solid State Chem.* **2000**, *152*, 3–20.
- Kanatzidis, M. G.; Sutorik, A. The Application of Polychalcogenide Salts to the Exploratory Synthesis of Solid State Multinary Chalcogenides at Intermediate Temperatures. *Prog. Inorg. Chem.* **1995**, *43*, 151–265.
- Yaghi, O. M.; O'Keeffe, M.; Ockwig, N. W.; Chae, H. K.; Eddaoudi, M.; Kim, J. Reticular Synthesis and the Design of New Materials. *Nature* **2003**, *423*, 705–714.
- Ferraris, G.; Makovicky, E.; Merlino, S. *Crystallography of Modular Materials*; International Union of Crystallography Monographs on Crystallography, no. 15; Oxford University Press: Oxford, U.K., 2004.
- Lima-de-Faria, J.; Hellner, E.; Liebau, F.; Makovicky, E.; Parthé, E. Nomenclature of Inorganic Structure Types. Report of the International Union of Crystallography Commission on Crystallographic Nomenclature Subcommittee on the Nomenclature of Inorganic Structure Types. *Acta Crystallogr.* **1990**, *A46*, 1–11.
- Anderson, S.; Hyde, B. G. Twinning on the Unit Cell Level as a Structure-Building Operation in the Solid State. *J. Solid State Chem.* **1974**, *9*, 92–101.
- (a) Aurivillius, B. Mixed Oxides with Layer Lattices. I. Structure Type of $CaC_2Bi_2O_9$. *Ark. Kemi* **1949**, *1*, 463–480. (b) Frit, B.; Mercurio, J. P. The Crystal Chemistry and Dielectric Properties of the Aurivillius Family of Complex Bismuth Oxides with Perovskite-like Layered Structures. *J. Alloys Compd.* **1992**, *188*, 27–35.
- (a) Dion, M.; Ganne, M.; Tournoux, M. Nouvelles Familles de Phases $M'M''_2Nb_3O_{10}$ a Feuilletés "Perovskites". *Mater. Res. Bull.* **1981**, *16*, 1429–1435. (b) Dion, M.; Ganne, M.; Tournoux, M.; Ravez, J. Crystalline-Structure of the Ferroelastic Layered Perovskite $CsCa_2Nb_3O_{10}$. *Rev. Chim. Miner.* **1984**, *21*, 92–103. (c) Dion, M.; Ganne, M.; Tournoux, M. $M'(A_{n-1}Nb_nO_{3n+1})$ Ferroelastic Foliated Perovskites, Where $n=2,3$ and 4. *Rev. Chim. Miner.* **1986**, *23*, 61–69. (d) Jacobson, A. J.; Johnson, J. W.; Lewandowski, J. T. Interlayer Chemistry between Thick Transition-Metal Oxide Layers: Synthesis and Intercalation Reactions of $K[Ca_2Na_{n-3}Nb_nO_{3n+1}]$ ($3 \leq n \leq 7$). *Inorg. Chem.* **1985**, *24*, 3727–3729.
- (a) Andersson, S.; Sundholm, A.; Magnéli, A. Homologous Series of Mixed Titanium Chromium Oxides $Ti_{n-2}Cr_2O_{2n-1}$, Isomorphous with the Series Ti_nO_{2n-1} and V_nO_{2n-1} . *Acta Chem. Scand.* **1959**, *13*, 989–997. (b) Magnéli, A. Structure of the ReO_3 -type with Recurrent Dislocations of Atoms; 'Homologous Series' of Molybdenum and Tungsten Oxides. *Acta Crystallogr.* **1953**, *6*, 495–500.
- (a) Battle, P. D.; Burley, J. C.; Gallon, D. J.; Grey, C. P.; Sloan, J. Magnetism and Structural Chemistry of the $n=2$ Ruddlesden-Popper Phase La_3LiMnO_7 . *J. Solid State Chem.* **2004**, *177*, 119–125. (b) Breard, Y.; Michel, C.; Hervieu, M.; Nguyen, N.; Studer, F.; Maignan, A.; Raveau, B.; Bouree, F. The Oxycarbonates $Sr_4(Fe_{2-x}Mn_x)_{1+y}(CO_3)_{1.3y}O_{6(1+y)}$: Nano, Micro and Average Structural Approach. *J. Solid State Chem.* **2003**, *170* (2), 424–434. (c) Zhang, Z.; Greenblatt, M. Synthesis, Structure, and Properties of $Ln_nNi_3O_{10-\delta}$ ($Ln = La, Pr, Nd$). *J. Solid State Chem.* **1995**, *117*, 236–246. (d) Greenblatt, M. Ruddlesden-Popper $Ln_{n+1}Ni_nO_{3n+1}$ Nickelates: Structure and Properties. *Curr. Opin. Solid State Mater. Sci.* **1997**, *2*, 174–183.
- Hladyshkevich, E. I.; Krypyakevich P. I. Homologous Series Including the New Structure Types of Ternary Silicides. *Acta Crystallogr.* **1972**, *A28*, Suppl. S97.
- Lattner, S. E.; Kanatzidis, M. G. $REAu_4Al_8Si$: The End Member of a New Homologous Series of Intermetallics Featuring Thick $AuAl_2$ Layers. *Chem. Commun.* **2003**, *18*, 2340–2341.
- Zhuravleva, M. A.; Chen, X. Z.; Wang, X.; Schultz, A. J.; Ireland, J.; Kannewurf, C. R.; Kanatzidis, M. G. X-ray and Neutron Structure Determination and Magnetic Properties of New Quaternary Phases $RE_{0.67}Ni_2Ga_{5+n-x}Ge_x$ and $RE_{0.67}Ni_2Ga_{5+n-x}Si_x$ ($n = 0, 1$; $RE = Y, Sm, Gd, Tb, Dy, Ho, Er, Tm$) Synthesized in Liquid Ga. *Chem. Mater.* **2002**, *14*, 3066–3081.
- Pring, A.; Jercher, M.; Makovicky E. Disorder and Compositional Variation in the Lillianite Homologous Series. *Mineral. Mag.* **1999**, *63*, 917–926.
- Moelo, Y.; Jambor, J. L.; Harris, D. C. Tintinaite and Associated Sulfosalts in Tintina (Yukon) – The Crystallochemistry of the Kobellite Series. *Can. Mineral.* **1984**, *22*, 219–226.
- Mumme, W. G. A Note on the Occurrence, Composition and Crystal-Structures of Pavonite Homologous Series Members P-4, P-6 and P-8. *Neues Jahrb. Mineral., Monatsh.* **1990**, *5*, 193–204.
- (a) Swinnea, J. S.; Steinfink, H. The Crystal-Structure of β - $BaFe_2S_4$ – The 1st Member in the Infinitely Adaptive Series $Ba_n(Fe_2S_4)_n$. *J. Solid State Chem.* **1980**, *32*, 329–334. (b) Swinnea, J. S.; Steinfink, H. The Phase Relationship among Compounds $Ba_{1+x}Fe_2S_4$. *J. Solid State Chem.* **1982**, *41*, 114–123.
- Bakker, M.; Hyde B. G. A Preliminary Electron Microscope Study of Chemical Twinning in the System $MnS + Y_2S_3$, an Analog of the Mineral System $PbS + Bi_2S_3$ (Galena + Bismuthinite). *Philos. Mag.* **1978**, *A38*, 615–628.
- The word "design" is used carefully here, and we do not want to convey a false impression that full design of compounds is possible. Too many variables are involved that make it very difficult to arrive at a level where we can design anything at will. Therefore by design we mean a relatively basic level achievable within a relatively narrow set of conditions.
- Mrotzek, A.; Kanatzidis, M. G. "Design" in Solid-State Chemistry Based on Phase Homologies. The Concept of Structural Evolution and the New Megaserie $A_m[M_{1+l}Se_{2+l}l_{2m}[M_{2+l+n}Se_{2+3l+n}]$. *Acc. Chem. Res.* **2003**, *36*, 111–119.
- In general, the metal atoms can be extensively disordered over all metal sites in the different structures. However, the degree of mixed M'/M'' occupancy varies for each metal site. According to single-crystal structure refinements of the quaternary selenides, the divalent metals in general prefer the periphery of the $NaCl^{100}$ -type units. These positions ($M'1$, $M'2$, etc.) can show mixed occupancies of tri-, di-, and even monovalent atoms. Therefore, triple disorder can sometimes occur in these sites.
- Mrotzek, A.; Iordanidis, L.; Kanatzidis, M. G. $Cs_{1-x}Sn_{1-x}Bi_{9+x}Se_{15}$ and $Cs_{1.5-3x}Bi_{9.5+x}Se_{15}$: Members of the Homologous Superseries $A_m[M_{1+l}Se_{2+l}l_{2m}[M_{1+2+l+n}Se_{3+3l+n}]$ ($A =$ alkali metal, $M = Sn$ and Bi) Allowing Structural Evolution in Three Different Dimensions. *Chem. Commun.* **2001**, 1648–1649.
- Mrotzek, A.; Iordanidis L.; Kanatzidis, M. G. New Members of the Homologous Series $A_m[M_6Se_9]_m[M_{5+n}Se_{9+n}]$: The Quaternary Phases $A_{1-x}M'_{3-x}Bi_{11+x}Se_{20}$ and $A_{1+x}M'_{3-2x}Bi_{7+x}Se_{14}$ ($A = K, Rb, Cs$; $M' = Sn, Pb$). *Inorg. Chem.* **2001**, *40*, 6204–6211.

- (28) Chung, D.-Y.; Choi, K.-S.; Iordanidis, L.; Schindler, J. L.; Brazis, P. W.; Kannewurf, C. R.; Chen, B.; Hu, S.; Uher, C.; Kanatzidis, M. G. High Thermopower and Low Thermal Conductivity in Semiconducting Ternary K–Bi–Se Compounds. Synthesis and Properties of β - $K_2Bi_8Se_{13}$ and $K_{2.5}Bi_{8.5}Se_{14}$ and Their Sb Analogues. *Chem. Mater.* **1997**, *9*, 3060–3071.
- (29) Mrozek, A.; Chung, D.-Y.; Ghelani, N.; Hogan, T.; Kanatzidis, M. G. Structure and Thermoelectric Properties of the New Quaternary Bismuth Selenides $A_{1-x}M_{4-x}Bi_{11+x}Se_{21}$ (A=K and Rb and Cs; M=Sn and Pb) – Members of the Grand Homologous Series $K_m(M_6Se_9)_n(M_{5+n}Se_{9+n})$. *Chem.–Eur. J.* **2001**, *7*, 1915–1926.
- (30) Mrozek, A.; Chung, D.-Y.; Hogan, T.; Kanatzidis, M. G. Structure and Thermoelectric Properties of the New Quaternary Tin Selenide $K_{1-x}Sn_{5-x}Bi_{11+x}Se_{22}$. *J. Mater. Chem.* **2000**, *10*, 1667–1672.
- (31) Mrozek, A.; Kanatzidis, M. G. Design in Solid State Synthesis Based on Phase Homologies: $A_{1-x}Sn_{9-x}Bi_{11+x}Se_{26}$ (A=K, Rb, Cs) – a New Member of the Grand Homologous Series $A_m[M_6Se_9]_{m-7}[M_{5+n}Se_{9+n}]$ with $M=Sn$ and Bi. *J. Solid State Chem.* **2002**, *167*, 299–301.
- (32) The value of x in the general formulae, for example, $A_{1-x}M'_{3-x}Bi_{11+x}Se_{20}$, reflects the different degrees of mixed occupancy. Although crystallographically these are single phases, we find varying extents of disorder regarding the occupancy ratio of the metal and also positional disorder in the alkali atom sites.
- (33) Cordier, G.; Schäfer, H.; Schwidetzky, C. On $Cs_3Bi_7Se_{12}$, a New Layer Selenidobismutate (III). *Rev. Chim. Miner.* **1985**, *22*, 676–683.
- (34) Kanatzidis, M. G.; McCarthy, T. J.; Tanzer, T. A.; Chen, L.-H.; Iordanidis, L.; Hogan, T.; Kannewurf, C. R.; Uher, C.; Chen, B. Synthesis and Thermoelectric Properties of the New Ternary Bismuth Sulfides $KBi_{6.33}S_{10}$ and $K_2Bi_8S_{13}$. *Chem. Mater.* **1996**, *8*, 1465–1474.
- (35) Iordanidis, L. Investigation in Multinary Bismuth Chalcogenide Systems: Synthesis, Characterization and Thermoelectric Properties of Bismuth Chalcogenides. Ph.D. Dissertation, Michigan State University, East Lansing, MI, 2000.
- (36) Wang, Y.-C.; DiSalvo, F. J. Synthesis and Characterization of $Ba_3Bi_{6.67}Se_{13}$ and Its Filled Variants $Ba_3Bi_6PbSe_{13}$ and $Ba_3Bi_6SnSe_{13}$. *Chem. Mater.* **2000**, *12*, 1011–1017.
- (37) Kanatzidis, M. G.; Chung, D.-Y.; Iordanidis, L.; Choi, K.-S.; Brazis, P.; Rocci, M.; Hogan, T.; Kannewurf, C. Ternary Alkali Metal Bismuth Chalcogenides as Thermoelectric Materials. *Mater. Res. Soc. Symp. Proc.* **1999**, *545*, 233–246.
- (38) Kyratsi, T.; Chung, D.-Y.; Kanatzidis, M. G. Bi/Sb Distribution and Its Consequences in Solid Solution Members of the Thermoelectric Materials $K_2Bi_{8-x}Sb_xSe_{13}$. *J. Alloys Compd.* **2002**, *338*, 36–42.
- (39) Chung, D.-Y.; Kyratsi, T.; Kanatzidis, M. G. Unpublished results.
- (40) Mrozek, A.; Kanatzidis, M. G. Unpublished results.
- (41) Choi, K.-S.; Chung, D.-Y.; Mrozek, A.; Brazis, P.; Kannewurf, C. R.; Uher, C.; Chen, W.; Hogan, T.; Kanatzidis, M. G. Modular Construction of $A_{1+x}M_{4-2x}M'_{7+x}Se_{15}$ (A = K, Rb; M = Pb, Sn; M' = Bi, Sb): A New Class of Solid State Quaternary Thermoelectric Compounds. *Chem. Mater.* **2001**, *13*, 756–764.
- (42) Iordanidis, L.; Bilc, D.; Mahanti, S. D.; Kanatzidis, M. G. Impressive Structural Diversity and Polymorphism in the Modular Compounds AB_3Q_5 (A = Rb, Cs; Q = S, Se, Te). *J. Am. Chem. Soc.* **2003**, *125*, 13741–13752.
- (43) Wiegiers G. A.; Meerschaut, A. Misfit Layer Compounds $(MS)_nTS_2$ (M=Sn, Pb, Bi, rare-earth metals; T=Nb, Ta, Ti, V, Cr; $1.08 \leq n \leq 1.23$): Structures and Physical Properties. *Mater. Sci. Forum*, **1992**, *100 & 101*, 101–172.
- (44) Wiegiers, G. A. Misfit layer compounds: Structures and Physical Properties. *Prog. Solid State Chem.* **1996**, *24*, 1–139.
- (45) Chung, D.-Y.; Hogan, T.; Brazis, P.; Rocci-Lane, M.; Kannewurf, C. R.; Bastea, M.; Uher, C.; Kanatzidis, M. G. $CsBi_4Te_6$: A High Performance Thermoelectric Material for Low-Temperature Applications. *Science* **2000**, *287*, 1024–1027.
- (46) Chung, D.-Y.; Choi, K.-S.; Brazis, P.; Kannewurf, C. R.; Kanatzidis, M. G. in *Thermoelectric Materials 1998 – The Next Generation Materials for Small-Scale Refrigeration and Power Generation Applications*; Tritt, T. M., Kanatzidis, M. G., Mahan, G. D., Lyon, H. B., Jr., Eds.; Materials Research Society symposium proceedings, Vol. 545; Materials Research Society: Warrendale, PA; 1999; pp 65–74.
- (47) Hsu, K. F.; Chung, D.-Y.; Lal, S.; Mrozek, A.; Kyratsi, T.; Hogan, T.; Kanatzidis M. G. $CsMBi_3Te_6$ and $CsM_2Bi_3Te_7$ (M = Pb, Sn): New Thermoelectric Compounds with Low-Dimensional Structures. *J. Am. Chem. Soc.* **2002**, *124*, 2410–2411.
- (48) Hsu, K. F.; Lal, S.; Hogan, T.; Kanatzidis, M. G. $CsPb_3Bi_3Te_8$ and $CsPb_4Bi_3Te_9$: Low-Dimensional Compounds and the Homologous Series $CsPb_mBi_3Te_{5+m}$. *Chem. Commun.* **2002**, 1380–1381.

AR040176W